

Results of the Japan-US Joint VLBI Experiments
--Kashima Group Analyses

Tetsuro KONDO, Yukio TAKAHASHI and Kosuke HEKI

Kashima Space Research Center, Radio Research Laboratory
893-1 Hirai, Kashima, Ibaraki 314, Japan

1. Introduction

Kashima has participated in 13 big experiments since January, 1984 (Table 1) using the VLBI system called K-3 which was developed to be compatible with the Mark-III VLBI system by Radio Research Laboratory (RRL). The cross-correlation processing of two "system level experiments", the latter half of WPAC2 in 1984 and NPAC1 in 1985 were carried out at Kashima by using the K-3 correlation system. Other experiment data relating to Kashima were cross-correlated at Haystack Observatory. Data analyses such as baseline analyses have been performed by Kashima analysis group independently of GSFC group. In this paper, the results of baseline analyses are mainly reported. The possibility of detecting the plate motion is also discussed briefly.

2. Station position analysis

The weighted least squares method is used for the analysis. The station position, clock parameters and the zenith path length of atmosphere are selected as the adjustment parameters. The International Radio Interferometric Surveying (IRIS) data are used for the earth orientation parameters (EOP). The IRIS data give the EOP of every 5 days without smoothing correction. Therefore, the instantaneous value of UT1 is calculated from the IRIS data as follows;

$$\text{UT1} = \text{interpolated value of (IRIS UT1 data - shorter period term)} \\ + \text{shorter period term}$$

where the shorter period term is a theoretically calculated value using the tidal terms with periods less than 35 days in Yoder's table (Yoder et al. , 1981).

Table 2 shows the source positions used in the analyses. These data are provided by the National Geodetic Survey(NGS) and used for obtaining the IRIS data, so that the self-consistency between the EOP and the source positions is kept in our analyses.

Table 3 summarizes the a-priori station positions with respect to the VLBI coordinate system, which is defined with its reference point at Haystack Observatory. In this table, the position of Kashima is derived from the results of land surveying conducted by the Geographical Survey Institute (GSI), Japan. The land surveying results are positions referred to the Besselian geodetic coordinate system adopted in Japan. Transformation from the Besselian system (x_B, y_B, z_B) to the VLBI geodetic coordinate system (x_V, y_V, z_V) then must be performed and it can be achieved through

the WGS72 coordinate system. The relation between these two coordinate systems is simply expressed by the form of a matrix equation.

$$\begin{pmatrix} x_V \\ y_V \\ z_V \\ 1 \end{pmatrix} = \begin{pmatrix} \alpha_V \cos \theta_V & \alpha_V \sin \theta_V & 0 & \alpha_V (\Delta X_B \cos \theta_V + \Delta Y_B \sin \theta_V) \\ -\alpha_V \sin \theta_V & \alpha_V \cos \theta_V & 0 & \alpha_V (-\Delta X_B \sin \theta_V + \Delta Y_B \cos \theta_V) \\ 0 & 0 & \alpha_V & \alpha_V \Delta Z_B + \Delta Z_V \\ 0 & 0 & 0 & 1 \end{pmatrix} \begin{pmatrix} x_B \\ y_B \\ z_B \\ 1 \end{pmatrix} \quad (1)$$

$$\begin{aligned} \text{where } \Delta X_B &= -140.0 \text{ m}, & \theta_V &= -0.54'' \\ \Delta Y_B &= 516.0 \text{ m}, & \alpha_V &= 1 + 0.3263 \times 10^{-6} \\ \Delta Z_B &= 673.0 \text{ m}, & \Delta Z_V &= 4.0 \text{ m} \end{aligned}$$

This matrix can be derived from combining two steps of coordinate transformation, i. e. the first is the conversion from Besselian system to WGS72 system and the second is from WGS72 to the VLBI coordinate system. $\Delta X_B, \Delta Y_B, \Delta Z_B$ are the shift of origin between Bessel system and WGS72 system and θ_V, α_V and ΔZ_V are Z-axis rotation angle, scaling factor and the offset of Z-components between WGS72 and the VLBI coordinate system, respectively.

The Marini model is normally used for the atmospheric model, which includes the effects of both dry and wet components. For the first half of WPAC2 and POLAR1 in 1984, we used the Chao model, because there were some stations where weather data acquisitions were imperfect. The excess path in magneto-ionic media (ionosphere and solar corona) is corrected by combining the S and X band data. The cable delay is also corrected by using cable delay counter data.

3. Principle of detecting the plate motion

According to the plate tectonics, the surface of earth is covered with a number of pieces of plate and each plate moves without internal deformation (see Fig. 1). The relative motion among these plates has been considered to cause a various tectonic phenomena and big earthquakes. The motion of each plate is conveniently described by using the Euler pole and rotation rate about the pole. These parameters can be derived from the ocean magnetic anomaly lineation, the direction of slip vector of the earthquakes and the azimuth of transform faults. Some investigators calculated the Euler pole and rotation speed from these data. In order to calculate the changing rate of the inter-plate baseline length, we used the model obtained by Minster and Jordan, 1978 (Table 4). The deviation of the station position caused by the plate motion can be calculated by Equation(2), where θ, ϕ and α denote the latitude and longitude of Euler pole and rotation angle, respectively.

$$\begin{pmatrix} X' \\ Y' \\ Z' \end{pmatrix} = \begin{pmatrix} A_{11} & A_{12} & A_{13} \\ A_{21} & A_{22} & A_{23} \\ A_{31} & A_{32} & A_{33} \end{pmatrix} \cdot \begin{pmatrix} X \\ Y \\ Z \end{pmatrix} \quad (2)$$

where

$$\begin{aligned} A_{11} &= \cos^2 \theta \cos^2 \phi (1 - \cos \alpha) + \cos \alpha \\ A_{12} &= \cos^2 \theta \cos \phi \sin \phi (1 - \cos \alpha) - \sin \theta \sin \alpha \\ A_{13} &= \cos \theta \sin \theta \cos \phi (1 - \cos \alpha) + \cos \theta \sin \phi \sin \alpha \\ A_{21} &= \cos^2 \theta \cos \phi \sin \phi (1 - \cos \alpha) + \sin \theta \sin \alpha \\ A_{22} &= \cos^2 \theta \sin^2 \phi (1 - \cos \alpha) + \cos \alpha \\ A_{23} &= \cos \theta \sin \theta \sin \phi (1 - \cos \alpha) - \cos \theta \cos \phi \sin \alpha \\ A_{31} &= \cos \theta \sin \theta \cos \phi (1 - \cos \alpha) - \cos \theta \sin \phi \sin \alpha \\ A_{32} &= \cos \theta \sin \theta \sin \phi (1 - \cos \alpha) + \cos \theta \cos \phi \sin \alpha \\ A_{33} &= \sin^2 \theta (1 - \cos \alpha) + \cos \alpha \end{aligned}$$

The changing rate of baseline length has been calculated for the baselines between Kashima and other points on the Pacific plate, Indian plate and Eurasian plate. The recent hypothesis that Kashima belongs to the North American plate (Kobayashi, 1983; Nakamura, 1983) is adopted in the calculation (see Fig. 2). Obtained changing rates (cm/year) are plotted on the world map as the contour map (see Fig. 3). Furthermore, changing rates of baseline lengths for those relating to Kashima, Mojave, Kauai, Kwajalein, Vandenberg and Gilcreek are shown in Figure 4. As seen in these figures, the baseline length change exceeding 5cm a year is expected for several baselines, such as Kashima-Kauai (-7.7cm), Kashima-Kwajalein(-8.5cm), Gilcreek-Kauai (-5.0cm) and Gilcreek-Vandenberg (-5.2cm). Then considering the potential of VLBI, it is possible to detect the plate motion by comparing the results obtained from the experiments separated only by one year.

4. Results

The IRIS data are used for the EOP as described in section 2. Furthermore the interpolation correcting the shorter period tidal term is used for calculate the instantaneous value of UT1. By adopting this interpolation method, a scatter in the estimated X and Y components of station positions decreases as demonstrated in Figure 5. The final value of estimated Cartesian coordinates are shown in Table 5. From Figure 6 to Figure 9, each component is plotted for every experiment and every station. In these figures, open circles and solid circles denote the results of Kashima group analyses and that of Goddard group's (J. W. Ryan and C. Ma, 1985), respectively, and crossed bars show the formal errors. Characters labeled to each circle represent the experiments, e. g. S1, W1 and P1 are system level experiment 1, WPAC1 and POLAR1, respectively. Subscript numbers 1 and 2 mean the first half and the latter half of an experiment in the case that we have analyzed the experiment by deviding it into two sessions.

The results of our analysis can not be directly compared with that of Goddard group from these figures because the models adopted in the analyses are different from one another, e. g. , Goddard group uses the BIH data for the EOP but the IRIS data are used in our case and the position of Mojave station was fixed in our case. In spite of these differences in the models, both group results except for Kwajalein and for X-component of Kashima coincide with one another within the range of several tens of centimeters. Large scattering in X-component of Kashima is thought to be due to the direction of baseline vector, i. e. , the baseline vectors from Kashima to other stations are almost parallel with the Y-axis so that the error included in the EOP mainly influences the X-component of Kashima.

By the way, as the EOP essentially contributes only to the coordinate rotation, it does not affect the baseline length. We actually got the good coincidence between both group results of baseline lengths as shown in Figure 10. In spite of the length of about 8000km, the discrepancy is only 3cm. Baseline lengths determined by Kashima group for the experiments conducted in 1984 are summarized in Table 6.

This year, 1985, Kashima has already participated in 7 experiments. The analysis of NPAC1 in 1985 has been progressing. Figure 11 shows the observed change of baseline lengths with respect to the results by the last year as the function of expected value of baseline change. If the plate moves like a model given in section 3, the observed change should be aligned on the broken line in this figure. Actually good correlation can be seen between expected value and observed one. Although this is a preliminary result, it is considered that the plate motion might be successfully detected.

5. Conclusions

The results of baseline analyses of Kashima group have been described. As described above, we can determine the baseline lengths between Kashima and other foreign stations with the error of about 3cm or better. Hence the plate motion it will be successfully detected by the end of this year, 1985. However much data are required to discuss the whole aspects of the plate motion. Therefore it is important to continue the observations using the VLBI technique for a long time at least ten years.

Acknowledgement

We would like to express our great appreciation to NASA/GSFC, Haystack and NGS staffs for kind cooperation and providing the data.

References

Kobayashi, Y., On the initiation of subduction of plates, *The Earth Monthly*, 5, 510-514, 1983 (in Japanese).

- Minster, J. B. and T. H. Jordan, Present-day plate motions, *J. Geophys. Res.*, 83, 5331-5354, 1978.
- Nakamura, K., Possible nascent trench along the eastern Japan Sea as the convergent boundary between Eurassian and North American plates, *Bull. Earthq. Res. Inst.*, 58, 711-722, 1983 (in Japanese).
- Ryan, J. W. and C. Ma, Crustal Dynamics Project Data Analysis - Fixed Station VLBI Geodetic Results, NASA TM-86229, 1985.
- Seno, T., Is northern Honshu a microplate?, *Tectonophysics*, 115, 177-196, 1985.
- Yoder, C. F., J. G. Williams, and M. E. Parke, Tidal variations of earth rotation, *J. Geophys. Res.*, 86, 881-891, 1981.

Table 1. Japan-US joint VLBI experiments (1984. 1 - 1985. 12).

Table 2. A priori source positions.

Table 3. A priori station positions on the VLBI coordinate system.

Table 4. Plate motion model.

Table 5. Estimated station positions.

Table 6. Observed baseline length in 1984.

Figure 1. Plates on the earth.

Figure 2. Position of Kashima in Japan.

Figure 3. Calculated changing rate of the baseline between Kashima and other points on Pacific plate, Indian plate, and Eurasian plate.

Figure 4. Expected rate of baseline length change.

Figure 5. A difference in the estimated X and Y components of Kashima due to the difference in the interpolation of UT1.

(a) : no short period term correcting case

(b) : short period term correcting case.

Figure 6. Estimated position of Kashima.

(a) : X and Y components

(b) : Horizontal and Z components

Figure 7. Same as Fig.6 for Kauai.

Figure 8. Same as Fig.6 for Gilcreek.

Figure 9. Same as Fig.6 for Kwajalein.

Figure 10. Observed length of Kashima-Mojave baseline.

Figure 11. Observed baseline length changes and expected changes.

Table 1. Japan-US joint VLBI experiments (1984. 1 - 1985. 12).

JAPAN-US JOINT VLBI EXPERIMENT
(1984.1 - 1985.12)

EXPERIMENT	START(UT) YYMMDDHH	STOP(UT) YYMMDDHH	TAPE*/ STATION	STATION
SLE-1	84012300	84012400	48	KAS-MOJ
SLE-2	84022418	84022518	34	KAS-MOJ-HAT
WPAC-1	84072809	84073014	66	KAS-MOJ-KWA-KAU-GIL
WPAC-2	84080406	84080614	66	KAS-MOJ-KWA-KAU-GIL
POLAR-1	84083008	84083112	30	KAS-MOJ-HAY-WET-GIL-ONS
POLAR-2	84090206	84090312	30	KAS-MOJ-HAY-WET-GIL-ONS
NPAC-1	85051520	85051620	30	KAS-MOJ-HAT-KAU-VAN-GIL
POLAR-1	85061920	85062102	30	KAS-MOJ-WST-WET-GIL-ONS
EPAC-1	85070606	85070800	49	KAS-MOJ-KWA-KAU-GIL-VAN
WPAC-1	85072018	85072212	50	KAS-MOJ-KWA-KAU-GIL-VAN
EPAC-2	85072718	85072912	49	KAS-MOJ-KWA-KAU-GIL-VAN
WPAC-2	85081006	85081200	52	KAS-MOJ-KWA-KAU-GIL-VAN
NPAC-2	85093000	85100100	30	KAS-MOJ-HAT-KAU-VAN-GIL
POLAR-2	85112120	85112302	30	KAS-MOJ-WST-WET-GIL-ONS

SLE : System Level Experiment
 KAS : Kashima KWA : Kwajalein HAY : Haystack
 MOJ : Mojave KAU : Kauai WET : Wettzell
 HAT : Hatcreek GIL : Gilcreek ONS : Onsala
 VAN : Vandenberg WST : Westford

Table 2. A priori source positions.

SOURCE POSITION (J2000.0)

SOURCE NAME		RIGHT ASCENSION			DECLINATION		
IAU	ALTERNATE	H	M	S	D	M	S
0106+013		1	8	38.77111	1	35	.3206
0212+735		2	17	30.81312	73	49	32.6226
0224+671	4C67.05	2	28	50.05157	67	21	3.0307
0229+131		2	31	45.89407	13	22	54.7186
0234+285		2	37	52.40567	28	48	8.9917
0235+164		2	38	38.93006	16	36	59.2783
0300+470		3	3	35.24215	47	16	16.2776
0355+508	NRAO150	3	59	29.74724	50	57	50.1631
0420-014		4	23	15.80089	-1	20	33.0611
0528+134		5	30	56.41674	13	31	55.1510
0552+398		5	55	30.80560	39	48	49.1665
0742+103		7	45	33.05954	10	11	12.6899
0851+202	OJ287	8	54	48.87491	20	6	30.6418
0923+392	4C39.25	9	27	3.01389	39	2	20.8524
1144+402		11	46	58.29797	39	58	34.3073
1226+023	3C273B	12	29	6.6997	2	3	8.5994
1235-055	3C279	12	56	11.16652	-5	47	21.5244
1354+195		13	57	4.43661	19	19	7.3736
1404+286	OQ208	14	7	.39437	28	27	14.6891
1418+546		14	19	46.59708	13	20	23.6864
1502+106		15	4	24.97973	10	29	39.1957
1548+056		15	50	35.26917	5	27	10.4472
1637+574		16	38	13.45625	57	20	23.9790
1642+690		16	42	7.84825	68	56	39.7564
1641+399	3C345	16	42	58.80989	39	48	36.9942
1741-038		17	43	58.85609	-3	50	4.8141
1749+096		17	51	32.81846	9	39	.7315
1803+784		18	0	45.68383	78	28	4.0178
1928+738		19	27	48.49164	73	58	1.5724
2134+004	2134+00	21	36	38.58631	0	41	54.2157
2145+067		21	48	5.45859	6	57	38.6058
2200+420	VR422201	22	2	43.29128	42	16	39.9809
2216-038		22	18	52.03772	-3	35	36.8769
2251+158	3C454.3	22	53	57.74788	16	8	53.5630

Table 3. A priori station positions on the VLBI coordinate system.

A P R I O R I S T A T I O N P O S I T I O N

STATION	X (m)	Y (m)	Z (m)
MOJAVE	-2356169.15	-4646756.83	3668471.22
KASHIMA	-3997894.93	3276580.09	3724115.46
KAUAI	-5543844.50	-2054565.70	2387814.29
KWAJALEIN	-6143535.36	1363995.57	1034707.89
GILCREEK	-2281544.915	-1453645.749	5756994.220
HAYSTACK	1492406.691	-4457267.330	4296882.102
WETTZELL	4075541.906	931734.189	4801629.393
HATCREEK	-2523968.05	-4123507.27	4147753.18
ONSALAGO	3370608.089J	711916.4485	5349830.8416

Table 4. Plate motion model.

P L A T E M O T I O N M O D E L (A M 1 - 2)

PLATE	Absolute Rotation Vector		
	θ ($^{\circ}$ N)	ϕ ($^{\circ}$ E)	ω (deg/m.y.)
AFRC	18.76	-21.76	0.139
ANTA	21.85	75.55	0.054
ARAB	27.29	-3.94	0.388
CARB	-42.80	66.75	0.129
COCO	21.89	-115.71	1.422
EURA	0.70	-23.19	0.038
INDI	19.23	35.64	0.716
NAZC	47.99	-93.81	0.585
NOAM	-58.31	-40.67	0.247
PCFC	-61.66	97.19	0.967
SOAM	-82.28	75.67	0.285

(after Minster & Jordan, 1978)

Table 5. Estimated station positions.

KASHIMA

EXPERIMENT(1984)	X-COMPONENT(m)	Y-COMPONENT(m)	Z-COMPONENT(m)
SLE1	-3997890.60 ± 0.03	3276580.29 ± 0.02	3724118.78 ± 0.03
SLE2	-3997890.41 ± 0.02	3276580.34 ± 0.02	3724118.72 ± 0.02
WPAC1-1	-3997890.87 ± 0.03	3276580.28 ± 0.02	3724119.10 ± 0.03
WPAC1-2	-3997890.78 ± 0.03	3276580.34 ± 0.02	3724118.93 ± 0.03
WPAC2-1	-3997890.45 ± 0.03	3276580.34 ± 0.02	3724118.74 ± 0.03
WPAC2-2	-3997890.50 ± 0.03	3276580.33 ± 0.02	3724118.67 ± 0.03
POLAR1	-3997890.63 ± 0.03	3276580.39 ± 0.02	3724118.92 ± 0.02
POLAR2	-3997890.57 ± 0.02	3276580.31 ± 0.02	3724118.85 ± 0.03
MEAN VALUE	-3997890.60 ± 0.16	3276580.33 ± 0.03	3724118.84 ± 0.14

KAUAI

EXPERIMENT(1984)	X-COMPONENT(m)	Y-COMPONENT(m)	Z-COMPONENT(m)
WPAC1-1	-5543844.45 ± 0.03	-2054565.47 ± 0.02	2387814.51 ± 0.02
WPAC1-2	-5543844.40 ± 0.02	-2054565.43 ± 0.02	2387814.44 ± 0.02
WPAC2-1	-5543844.19 ± 0.02	-2054565.30 ± 0.02	2387814.29 ± 0.02
WPAC2-2	-5543844.26 ± 0.03	-2054565.36 ± 0.02	2387814.27 ± 0.03
MEAN VALUE	-5543844.33 ± 0.12	-2054565.39 ± 0.08	2387814.38 ± 0.12

KWAJALEIN

EXPERIMENT(1984)	X-COMPONENT(m)	Y-COMPONENT(m)	Z-COMPONENT(m)
WPAC1-1	-6143535.15 ± 0.05	1363995.85 ± 0.02	1034708.12 ± 0.03
WPAC1-2	-6143535.21 ± 0.04	1363995.93 ± 0.02	1034708.03 ± 0.03
WPAC2-1	-6143534.76 ± 0.04	1363995.99 ± 0.02	1034707.81 ± 0.03
WPAC2-2	-6143534.99 ± 0.04	1363995.96 ± 0.02	1034707.77 ± 0.03
MEAN VALUE	-6143535.03 ± 0.20	1363995.93 ± 0.06	1034707.93 ± 0.17

GILCREEK

EXPERIMENT(1984)	X-COMPONENT(m)	Y-COMPONENT(m)	Z-COMPONENT(m)
WPAC1-2	-2281545.27 ± 0.02	-1453645.89 ± 0.02	5756993.80 ± 0.02
WPAC2-1	-2281545.18 ± 0.03	-1453645.88 ± 0.02	5756993.72 ± 0.04
WPAC2-2	-2281545.23 ± 0.03	-1453645.90 ± 0.02	5756993.75 ± 0.04
POLAR1	-2281545.21 ± 0.01	-1453645.89 ± 0.02	5756993.76 ± 0.04
POLAR2	-2281545.19 ± 0.01	-1453645.91 ± 0.02	5756993.75 ± 0.03
MEAN VALUE	-2281545.22 ± 0.04	-1453645.89 ± 0.01	5756993.76 ± 0.03

Table 6. Observed baseline length in 1984.

OBSERVED BASELINE LENGTHS (MEAN VALUE)

BASELINE	LENGTH (m)	EXPERIMENTS(1984)
KASHIMA - MOJAVE	8091824.13±0.04	SLE1,SLE2,WPAC1,WPAC2,POLAR1,POLAR2
* KASHIMA - KAUAI	5709360.48±0.04	WPAC1,WPAC2
* KASHIMA - KWAJALEIN	3936330.78±0.04	WPAC1,WPAC2
KASHIMA - GILCREEK	5427104.40±0.02	WPAC1,WPAC2,POLAR1,POLAR2
KASHIMA - HAYSTACK	9501780.07±0.05	POLAR1,POLAR2
KASHIMA - WETTZELL	8475827.14±0.04	POLAR1,POLAR2
* MOJAVE - KAUAI	4303581.24±0.02	WPAC1,WPAC2
* MOJAVE - KWAJALEIN	7576938.57±0.06	WPAC1,WPAC2
MOJAVE - GILCREEK	3816209.19±0.02	WPAC1,WPAC2
MOJAVE - HAYSTACK	3904144.28±0.01	POLAR1,POLAR2
MOJAVE - WETTZELL	8588976.48±0.03	POLAR1,POLAR2
KAUAI - KWAJALEIN	3725196.31±0.04	WPAC1,WPAC2
* KAUAI - GILCREEK	4728114.79±0.03	WPAC1,WPAC2
GILCREEK - HAYSTACK	5039482.23±0.01	POLAR1,POLAR2
GILCREEK - WETTZELL	6856771.52±0.02	POLAR1,POLAR2
HAYSTACK - WETTZELL	5997390.80±0.04	POLAR1,POLAR2
KWAJALEIN - GILCREEK	6719676.67±0.08	WPAC1,WPAC2

* : Baseline suitable for detecting the plate motion.

PLATES ON THE EARTH

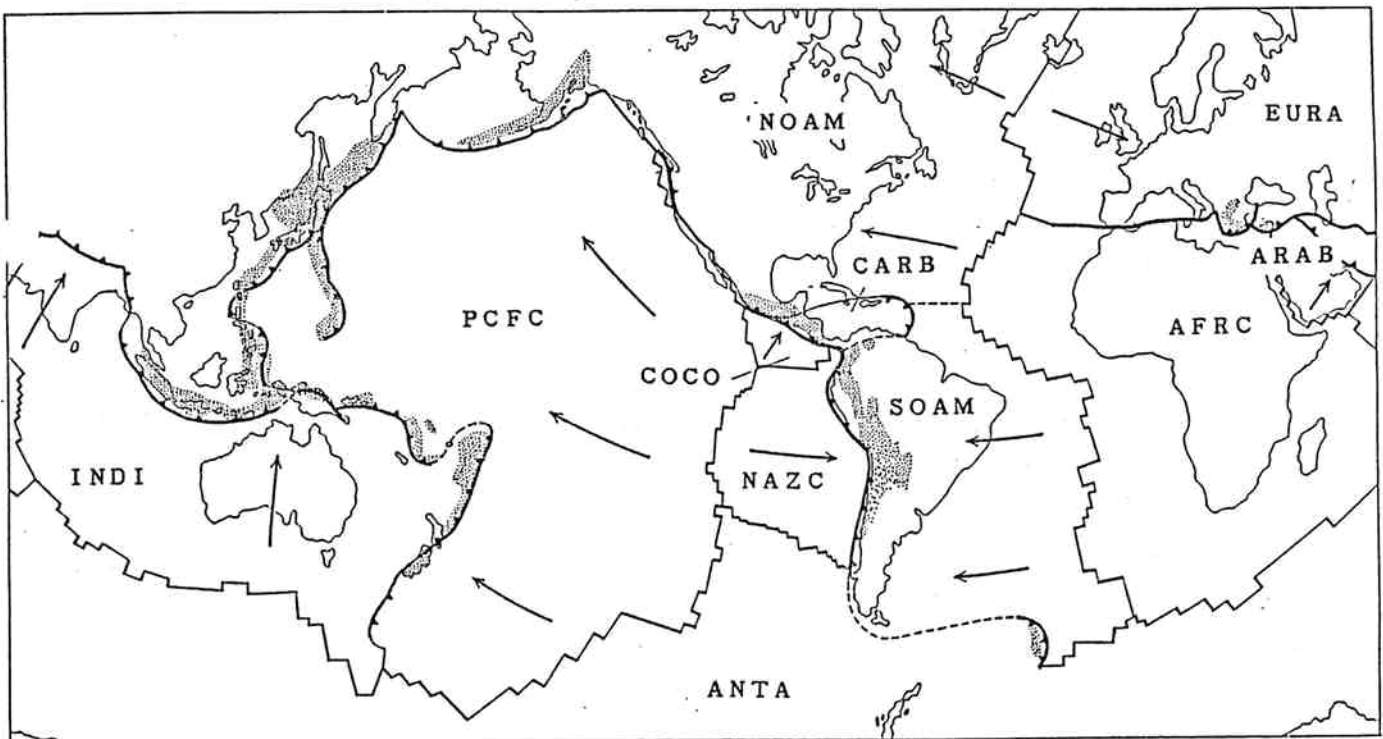
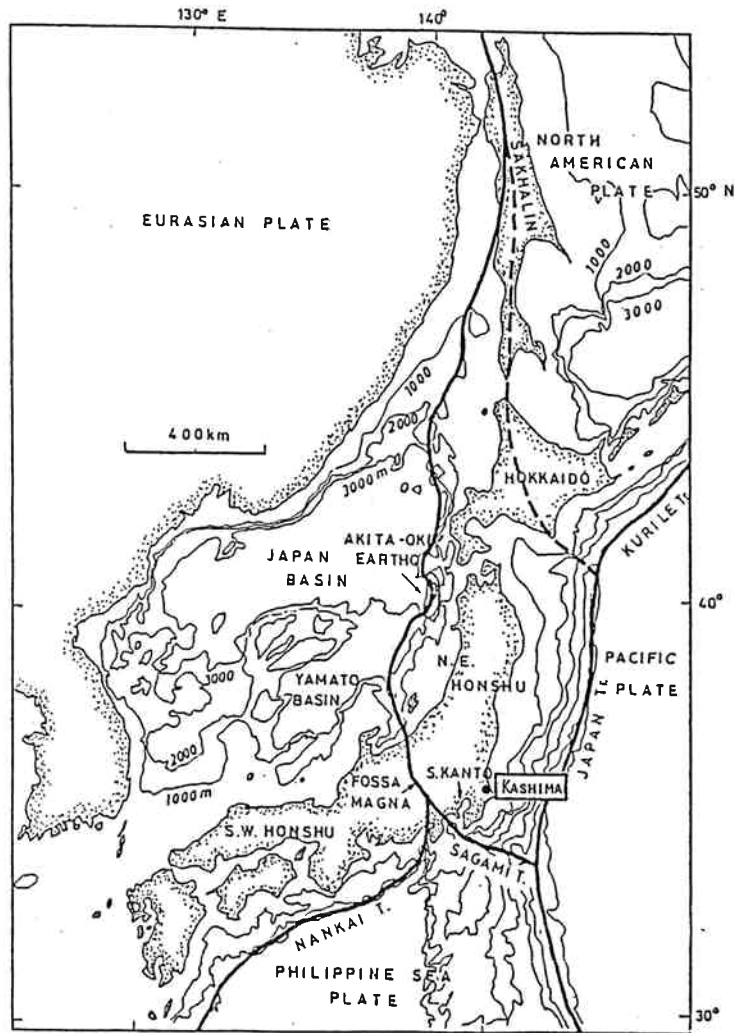


Figure 1. Plates on the earth.



(after Seno, 1985)

Figure 2. Position of Kashima in Japan.

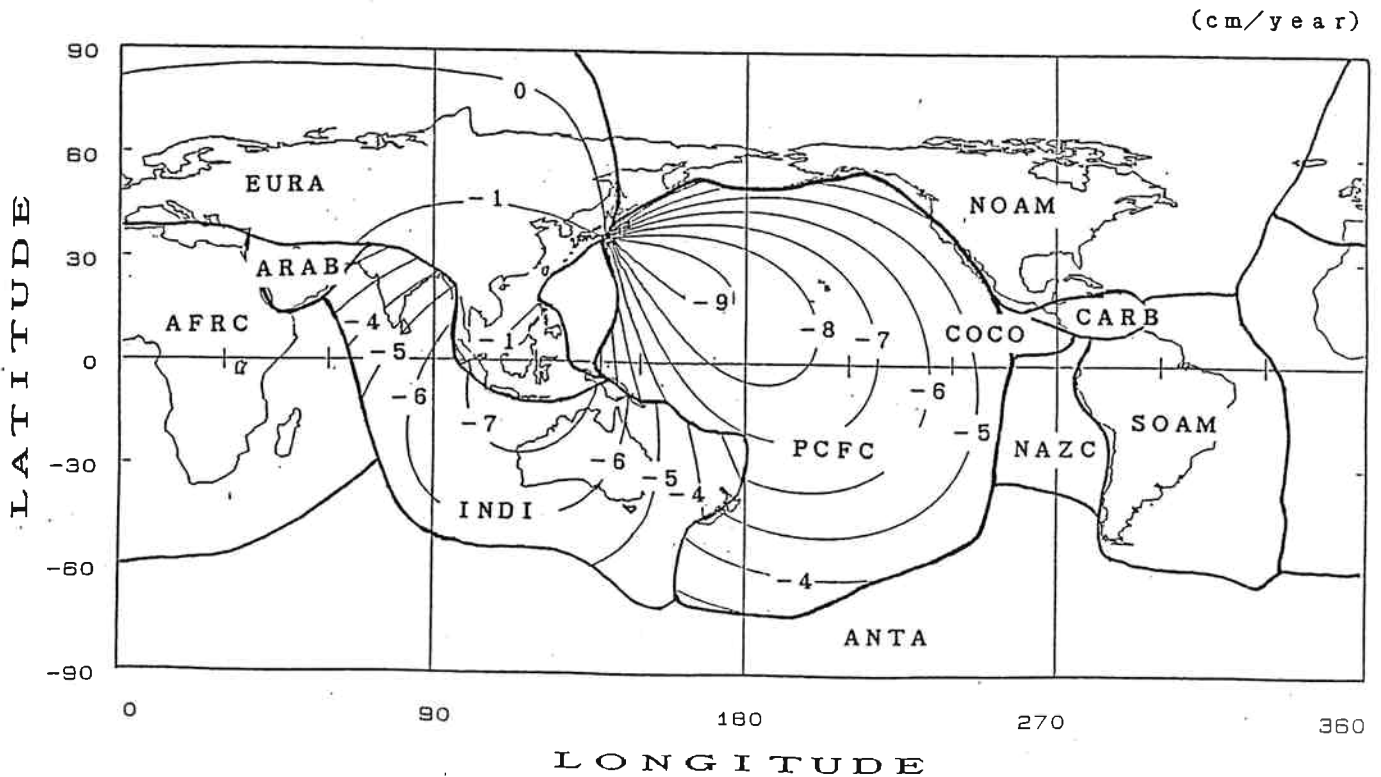


Figure 3. Calculated changing rate of the baseline between Kashima and other points on Pacific plate, Indian plate, and Eurasian plate.

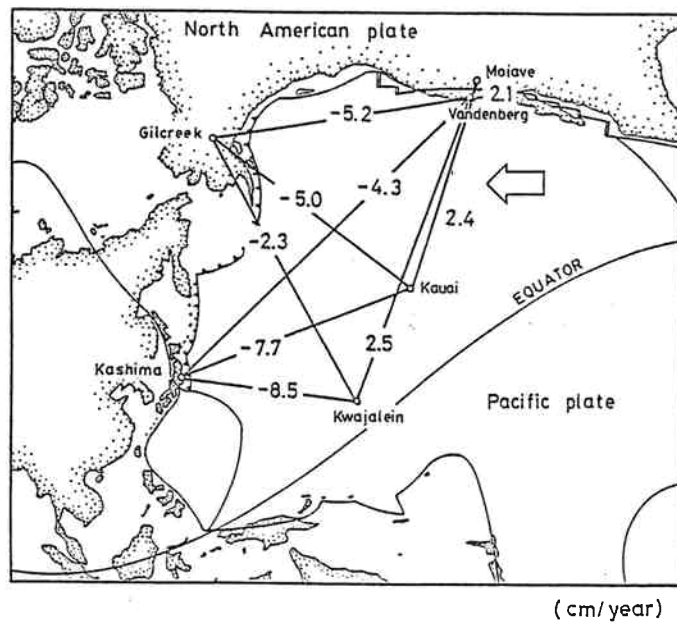
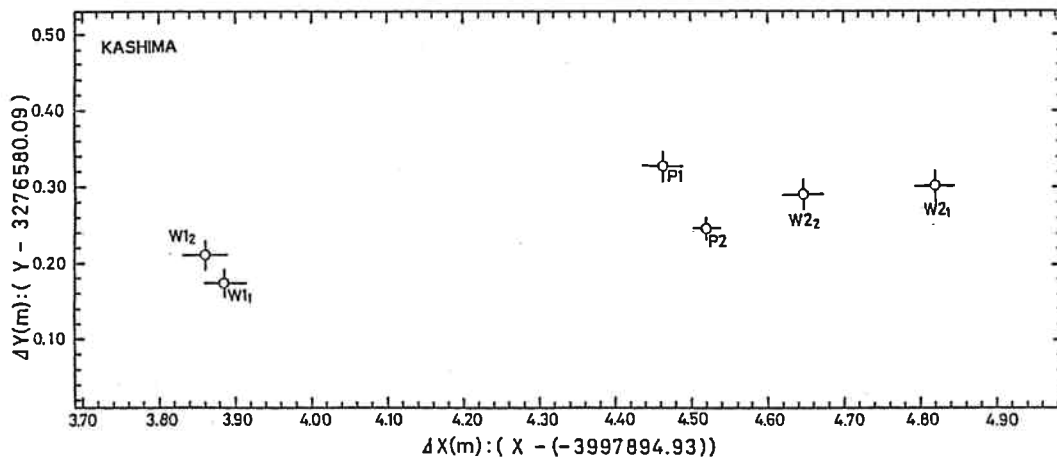


Figure 4. Expected rate of baseline length change.

(a) UT1 INTERPOLATION : NO SHORT PERIOD TERM CORRECTING CASE



(b) UT1 INTERPOLATION : SHORT PERIOD TERM CORRECTING CASE

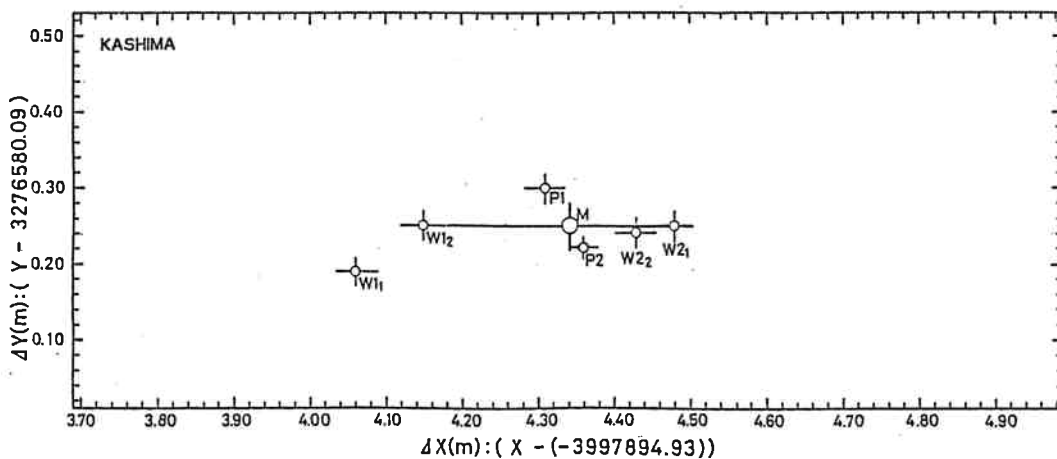


Figure 5. A difference in the estimated X and Y components of Kashima due to the difference in the interpolation of UT1.
 (a) : no short period term correcting case
 (b) : short period term correcting case.

